Interannual lake fluctuations in the Argentine Puna: relationships with its associated peatlands and climate change

Elvira Casagranda, Carlos Navarro, H. Ricardo Grau & Andrea E. Izquierdo

Regional Environmental Change

ISSN 1436-3798
Volume 19
Number 6

Reg Environ Change (2019)
19:1737-1750
DOI 10.1007/s10113-019-01514-7

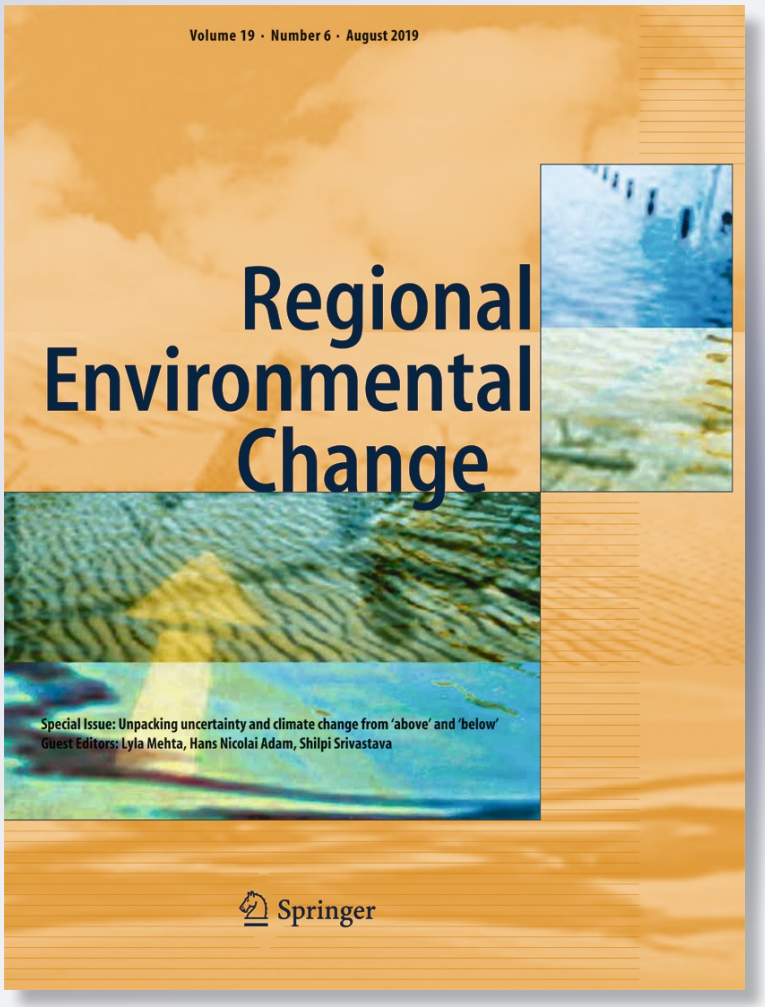

Springer

Regional Environmental Change (2019) 19:1737–1750
https://doi.org/10.1007/s10113-019-01514-7

ORIGINAL ARTICLE

Interannual lake fluctuations in the Argentine Puna: relationships with its associated peatlands and climate change

Elvira Casagranda[1] · Carlos Navarro[1] · H. Ricardo Grau[1] · Andrea E. Izquierdo[1]

Received: 28 November 2018 / Revised: 18 April 2019 / Accepted: 7 May 2019 / Published online: 27 May 2019

Abstract

High elevation ecosystems are likely more sensitive to climate change. But, due to paucity of instrumental records, such effects are poorly studied, particularly in mountains outside Europe and North America. Here, we quantified water body area fluctuations for the last 32 years in 15 lakes spread over an area of 14.3 million ha in the Argentine Puna, through the classification of Landsat images; and we quantified peatlands NDVI (a proxy of vegetation productivity) from MODIS images. We evaluated the pairwise similarity between lakes interannual fluctuations and their relationship with climate models (TRMM 3B43 v7; CRU TS 4.10) and potential controls (ENSO index); and the correlations between water body area and the NDVI variation of its associated peatlands. Lakes were grouped in two clusters defined by their synchronic water body area variability and these clusters define two main geographic zones: NE and SW. Consistent with previous observations of an overall aridization trend, water body area generally decreased but showed large variability among lakes. Peatlands productivity was more correlated with lake variability than with modeled precipitation, and lake water body area was weakly related to indices of ENSO, providing an additional tool to relate local climate with continental and global climate models. The analysis shows that lake behavior is highly variable spatially and temporally, and that satellite-based monitoring is a valuable tool for assessing ecological conditions of wetlands in the region, characterized by the lack of climatic instrumental records; and to explore the vulnerability of wetlands to climate change.

Keywords Puna · Lake · Water body area · Aridization · Peatlands · ENSO · Climate change

Introduction

Wetlands are key ecological functional units in high elevation deserts such as the Argentine Puna, where water is the most limiting life factor. Located from 3000 to more than 5000 m a.s.l., lakes and peatlands are the main types of wetlands in the region, hosting a great biological diversity with many endemic plant and animal species (Mittermeier et al. 2008). Although lakes and peatlands represent only 1.5% of the 14.3 million ha of the Argentine Puna total area (Izquierdo et al. 2015, 2016), they provide essential ecosystem services to human populations, livestock, and wildlife (Izquierdo et al. 2018). Peatlands are important regional carbon sinks (Kusler et al. 1994) and play a key role in high-elevation environments by maintaining water regulation and forage provision for native and exotic herbivores (Villagrán and Castro 1997; Squeo et al. 2006; Meneses et al. 2015; Izquierdo et al. 2018). Lakes harbor bird species of high conservation value, such as flamingos, and, in consequence, the Ramsar Initiative has declared four "priority sites for conservation of the avifauna" in the region (https://www.ramsar.org/es/humedal/argentina). Also, the importance of these wetlands for the maintenance of microbial communities of high scientific value has been recently demonstrated (Farías et al. 2013).

Puna wetlands are spatially and temporally variable due to natural, and particularly for peatlands, anthropogenic

Editor: Juan Ignacio Lopez Moreno

Electronic supplementary material The online version of this article (https://doi.org/10.1007/s10113-019-01514-7) contains supplementary material, which is available to authorized users.

✉ Elvira Casagranda
elvira.casagranda@gmail.com

Carlos Navarro
carlos-n@outlook.com

H. Ricardo Grau
chilograu@gmail.com

Andrea E. Izquierdo
aeizquierdo@gmail.com

[1] Instituto de Ecología Regional and Consejo Nacional de Investigaciones Científicas y Técnicas (CONICET), Universidad Nacional de Tucumán, CC 34, 4107 Yerba Buena, Tucumán, Argentina

causes. Climate characteristics include intensive droughts, strong winds, high irradiation, and extreme thermal amplitudes (Caziani and Derlindati 1999; Carilla et al. 2013). This climate variability is probably the greatest driver of wetland fluctuation and may increase due to the current trend towards drier conditions (Carilla et al. 2013; Morales et al. 2015), a concept that in this work we will refer to as aridization; and to the fact that high mountains are especially sensitive to climate change (Beniston et al. 1997; Beniston 2003; Beniston 2005). During the past century, persistent warming trends have been reported in the tropical and subtropical Andes (Vuille et al. 2000). Models of atmospheric circulation suggest that global warming will probably cause changes in the amount and intensity of precipitation, and an increased risk of drought in the Andes (Haylock et al. 2006; Liebmann et al. 2007), with longer dry seasons (Buytaert et al. 2010) and temperature rises at higher elevation (Urrutia and Vuille 2009; Morales et al. 2018). In addition, El Niño-Southern Oscillation (ENSO), the strongest natural interannual climate phenomenon fluctuation that originates in the tropical Pacific Ocean (Philander 1989), has large effects on ecological systems at a global scale, and also influences the entire global climate system (Glantz et al. 1991). Although certain studies have addressed ENSO responses to global climate change (Yeh and Kirtman 2007, Power et al. 2013), there are still uncertainties about it (Latif and Keenlyside 2009).

Despite the aridization trends found in the Puna (Carilla et al. 2013; Morales et al. 2015), the effects of climate change on wetlands are still poorly understood. Since the Puna is a region of endorheic watersheds (Paoli et al. 2002), lake water body area is expectedly very sensitive to water inputs and outputs (Lupo et al. 2007; Carilla et al. 2013; Morales et al. 2015). Therefore, fluctuations in lake water body area are a potential *proxy* for water balance variations, particularly considering the scarcity of instrumental records in the region (Carilla et al. 2013).

Satellite images like the Landsat mission (30 m pixel resolution) provide an effective tool for monitoring and detecting temporal changes in lakes, due to their wide coverage, multispectral information and relative short revisit period (16 days). Variations in lake water body area can be measured using Landsat 5 Thematic Mapper (TM) satellite images (Caziani and Derlindati 1999; Carilla et al. 2013), available since 1984, and it is possible to create multidecadal time series that reach recent dates using images of the Landsat 7 Enhanced Thematic Mapper Plus (ETM+), and Landsat 8 Operational Land Imager (OLI) satellites. In addition, measures of estimated precipitation and temperature can be obtained through the Tropical Rainfall Measuring Mission (TRMM; 0.25° × 0.25° spatial resolution), and through the Climatic Research Unit (CRU) Time-Series (TS) climate dataset (0.5° × 0.5° spatial resolution) respectively, which can be compared with lake water body area variations. Peatlands are characterized by their high productivity, which allows mapping them relatively easily through satellite images due to its contrast with the surrounding arid matrix (Squeo et al. 1993, 2006; Izquierdo et al. 2015, 2016). This feature allows to analyze seasonal changes in vegetation indices (e.g., NDVI) using Moderate-Resolution Imaging Spectroradiometer (MODIS) satellite products.

The goals of this study were (1) to quantify the interannual water body area variation of 15 lakes spread over the Argentine Puna between 1986 and 2017; (2) to identify trends in each lake water body area and geographical patterns of lakes with similar interannual water body area variation; (3) to evaluate the relationship between lake water body area with productivity of its associated peatlands; and (4) to relate annual lake water body area with precipitation, mean annual temperature, and ENSO indices, for describing climatic influence on wetlands. Advances in the knowledge of the interactions between these variables and the main wetlands of these high elevation deserts, where water is the limiting resource, will provide tools for the conservation and sustainable development of the region, as it will also help predict the response and vulnerability of these wetlands to scenarios of climate change.

Methods

Study area

This study includes the Puna ecoregion in northwestern Argentina, covering an area of approximately 14.3 million ha (Izquierdo et al. 2015) (Fig. 1). The area is delimited to the North, West, and South by the limits between Argentina and Bolivia, Argentina and Chile, and the southern boundary of San Guillermo Biosphere Reserve in San Juan province, respectively; while the eastern limit is given by the contour line of 3200 m a.s.l (Izquierdo et al. 2015). In the ecoregion, 866,580 ha of wetlands were reported of which 40,486 ha correspond to lakes and 895 ha to peatlands, while the remaining are salt flats (Izquierdo et al. 2016). The ecoregion is characterized by its aridity, with average annual rainfall of less than 400 mm concentrated in summer (Cabrera 1976; Morales et al. 2018), and which decreases in northeast-southwest direction up to sectors with less than 100 mm of annual rainfall (Reboratti 2005). In general terms, the climate in the Puna and the High Andes is regulated by two systems. One is the geographical position and intensity of the high-pressure center "Alta" of Bolivia or Bolivian High, which causes greater rainfall the further south it moves. The other is the weakening of the tropical winds from the west over the Central Andes, which promotes masses of moist air to enter from the east,

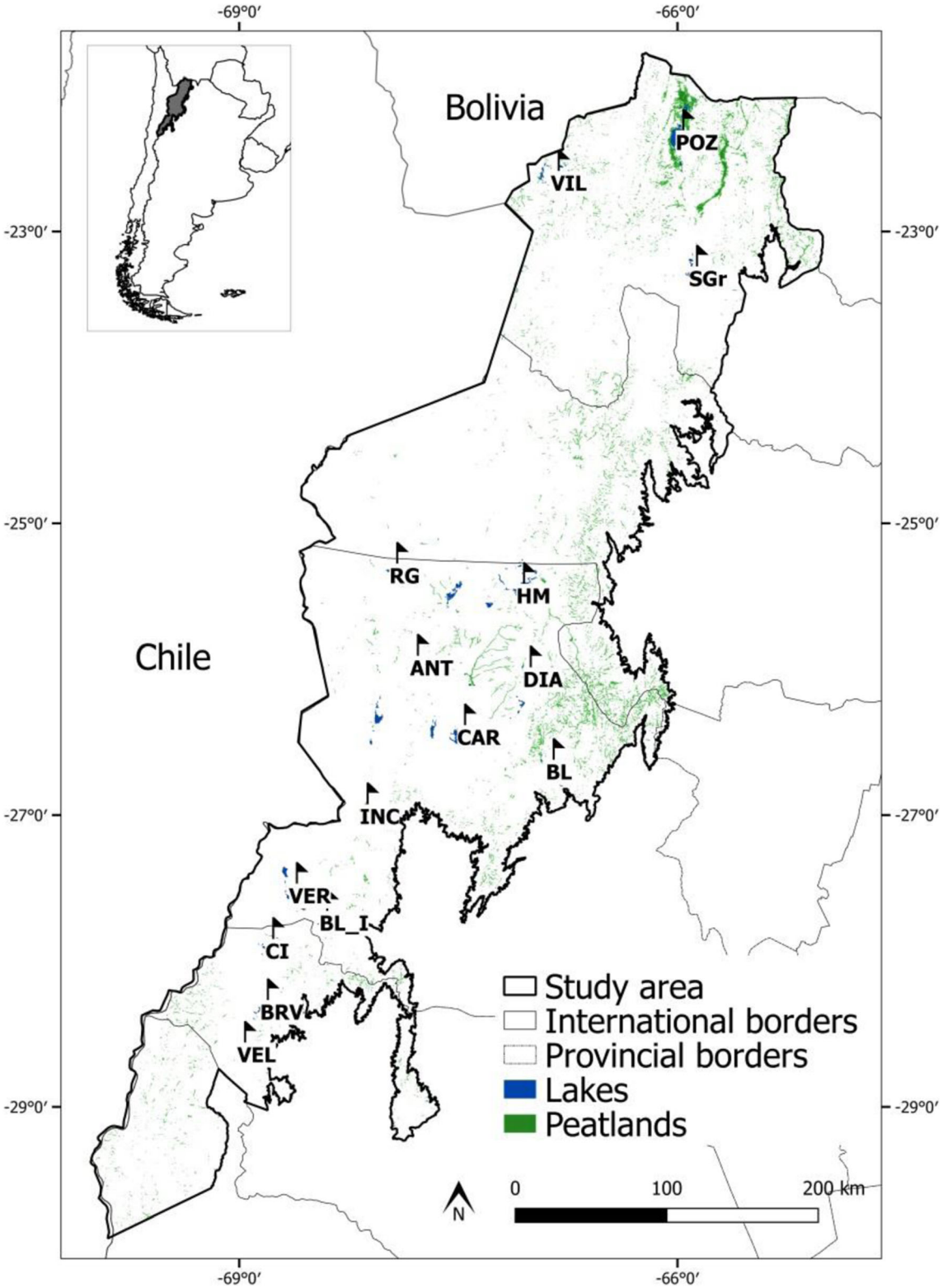

Fig. 1 Study area map with lakes location: 1. Pozuelos (POZ) 2. Vilama (VIL) 3. Salinas Grandes (SGr) 4. Río Grande (RGr) 5. Hombre Muerto (HM) 6. Diamante (DIA) 7. Carachipampa (CAR) 8. Antofalla (ANT) 9. Laguna Blanca (BL) 10. Incahuasi (INC) 11. Laguna Verde (VER) 12. Laguna Blanca I (BL_I) 13. Corona del Inca (CI) 14. Laguna Brava (BRV) 15. Veladero (VEL)

generating episodes of higher humidity (Garreaud and Aceituno 2001; Vuille and Keimig 2004). Several studies report that a significant fraction of precipitation interannual variability in the High Andes is associated with the ENSO

phenomenon (Vuille et al. 2000; Garreaud and Aceituno 2001); showing a tendency towards wet conditions during the cold phase (La Niña events), and dry conditions during the warm phase (El Niño events).

Lake selection

We studied 15 lakes for a 32-year period (1986–2017). Lakes included in this study were previously identified in the wetland mapping of the Argentinian Puna (Izquierdo et al. 2016). We chose the 10 largest lakes and 5 more to improve the spatial coverage of the entire geographical area. The lake map generated by Izquierdo et al. (2016) was developed through the classification of a multitemporal mosaic of Landsat images between February–April 2009 and 2013. In our study time period (1986–2017), selected lake ranges in water body area from 28 to 7000 ha (calculated as the average lake water body area for that period) are located in an altitudinal range from 3000 to 5500 m a.s.l. and are in general shallow lakes (Table 1).

Imagery acquisition and processing

To analyze changes in lake water body area, we used Landsat images (30 m spatial resolution) with different sensors covering the entire period: Landsat 5 TM images were used for the periods 1986–1999 and 2004–2011; Landsat 7 ETM+ for the 2000–2003 period and year 2012; and Landsat 8 OLI for the 2013–2017 period.

Table 1 Lakes variables: average water body area (1986–2017), altitude, and average depth. Average depth variable was extracted from http://www.hydrosheds.org (Messager et al. 2016)

Lakes	Average water body (ha)	Altitude (m a.s.l.)	Average depth (m)
Pozuelos	6875	3659	2.6
Vilama	2797	4811	6
Salinas Grandes	1360	3405	1.3
Rio Grande	32	4028	2.5
Hombre Muerto	1397	3970	4.2
Antofalla	410	4571	2.6
Diamante	1067	3010	6.4
Carachipampa	463	3738	1.4
Laguna Blanca	542	3199	4.1
Incahuasi	189	4002	2.5
Laguna Verde	3430	4161	7.3
Laguna Blanca I	111	4279	5.3
Corona del Inca	334	5495	13
Laguna Brava	1128	4261	3.4
Veladero	28	3954	4.6

Image analysis was done through Google Earth Engine (GEE) platform (https://earthengine.google.com/), a cloud-based free access archive that provides massive satellite data collection, including almost all of the Landsat imagery. We used images scenes calibrated to top-of-atmosphere (TOA) reflectance, and orthorectified. The TOA products generated by GEE algorithms are obtained with an Earth Engine specific method that uses stored coefficients in each scene metadata (Chander et al. 2009), accounting for solar elevation and seasonally variable Earth-Sun distance. The main image selection criteria in GEE were (1) images belonged to the period January–May of each year, to represent the rainy season (to measure water body area when they have received the summer precipitations-the most substantial portion of the annual fall), and (2) had less than 40% of cloud cover, since with a lower cloud cover limit certain scenes were not available in many of the years. As a result, for each of the years, the number of images available varied between 30 and more than 100. Finally, on the resulting images set of in each year, a statistical median was applied to all the bands of each image (except the thermal band), to resume the summer information in a single median image per year. We considered the median as the best measure since it is less affected by extreme values that may exist in the data (Kayastha et al. 2012; Müller et al. 2015). Additionally, through the Global Surface Water platform (https://global-surface-water.appspot.com/), it is possible to check the intra-annual variability of the lakes here studied; finding that between January and May the changes in water body area are generally minor, which supports the use of the median to obtain the annual images. In each of the resulting images, NDVI of the entire scene was calculated using the corresponding bands according to the type of product used (i.e., bands 4 and 3 for TM and ETM+, and bands 5 and 4 for OLI).

Lake water body area delimitation

To determine annual lake water body area, we classified each annual image using the non-parametric method Support Vector Machine (SVM) (Hsu et al. 2007), through GEE. This method is routinely used in remote sensing due to its ability to successfully administer small sets of training data, often producing greater accuracy in classification than other methods (Mantero et al. 2005). SVM minimizes data misclassification without preconceived ideas about its probability distribution. We used samples visually obtained from Google Earth high resolution images to train the classifier and subsequent validation of the classifications, aiming at discriminating only two spectral classes: "water" and "not water", with the latter including all other types of cover.

We performed the SVM classifications using the previously generated NDVI band, and band 5 (in TM and ETM+) or band 6 (in OLI) as inputs, since these bands gave the best

results when discriminating water from the other coverages (i.e., bare soil, vegetation) in this study. Lee et al. (2001) showed that the Landsat TM and ETM+ band 5 best separates the water-soil boundary, since it is the least sensitive to water sediment load. On the other hand, NDVI (values between − 1 and 1) is capable of extracting water surfaces with good results (Rokni et al. 2014).Water pixels in NDVI "band" take values approaching − 1, differentiating themselves from the rest of the coverages. Of 32 classifications, in 29, the accuracy and Kappa index equaled 1, while in the other 3 the accuracy and the Kappa index varied between 0.87 and 0.9, and 0.72 and 0.88, respectively. The Kappa statistic takes values between 0 and 1, indicating a full agreement between reality and the map when it is close to 1, whereas values close to 0 suggest that the observed arrangement is very not discernible from chance. From each classified annual image, we extracted the water class, identified the lakes selected for the analyses and calculated the lake water body area.

Lake water body area fluctuations and cluster analysis

We calculated lake water body area fluctuations by subtracting water body area of each year from the previous one ($A_x - A_{x-1}$). To describe lake water body area fluctuations between 1986 and 2017, we report lake water body area range (ha), total and relative water body area change with respect to the start-up year of the series (water body $area_{2017}$ − water body $area_{1986}$), slope of water body area trend between 1986 and 2017, and water body area coefficient of variation (CV = standard deviation/mean) as a variability descriptor in each lake (Table 2). Relative water body area was calculated as annual water body area/maximum water body area during the 1986–2017 period.

To explore how water body area fluctuations of different lakes follow a common pattern, we performed a hierarchical clustering (HC; Ward 1963) analysis. HC finds hierarchies in the input data by generating groups based on the closeness or similarity in the data. Then, the closest pairs are calculated and, in an ascending way, groups of classes are generated. We measured the pairwise (dis) similarity between series of lake water body fluctuation using the Euclidean distance, and the distance between clusters was calculated implementing Ward's minimum variance method, which minimizes the total within-cluster variance. At each step, the pair of clusters with minimum between-cluster distance is merged until finding the optimal solution.

Peatland phenology

We analyzed peatland phenology based on the NDVI dynamics obtained through the analysis of MODIS images. Given that MODIS pixel size is larger than minimum area of peatlands (i.e., 1 ha), we used a spatial algorithm to estimate the sub-pixel contribution of the peatlands to NDVI. We used the MODIS data set to estimate the NDVI instead of the Landsat, due to its higher temporal resolution; as NDVI MODIS data proved to be correlated with the Landsat NDVI values. NDVI is an index based on vegetation reflectance in the red and infra-red wavelength bands, highly correlated with vegetation photosynthetic activity; and therefore routinely

Table 2 Lakes studied; minimum, and maximum water body area; net water body area change between 1986 and 2017; relative water body area change, slope of water body area trend (1986–2017); lake area CV; and *r* values for the correlations water body area/water body area fluctuation in each lake

Lakes	Area range (ha)	Net area change in 32 years (ha)	Relative area change	Regression slope (ha/year) (p value)	Lake area CV	Correlation lake area–lake area fluctuation
Pozuelos	0–13.500	− 12.495	− 0.925	− 24.2 (0.7)	0.54	− .44**
Vilama	648–5989	− 1049	− 0.175	− 53 (0.04)	0.50	− .50**
Salinas G.	0–8601	− 5538	− 0.643	11.4 (0.8)	1.79	− .61***
Rio Grande	13–77	7.3	0.095	− 0.2 (0.5)	0.47	− .74***
H. Muerto	137–4009	10	0.002	5.8 (0.7)	0.74	− .54**
Antofalla	0–803	575	0.716	10.8 (0.001)	0.37	− .60***
Diamante	733–1418	− 278	− 0.195	− 12.9 (0.0004)	0.19	− .32
Carachipampa	791–287	118	0.149	− 0.1 (0.9)	0.27	− .71***
L. Blanca	0–4305	− 38	− 0.008	5.9 (0.7)	1.54	− .57***
Incahuasi	20–358	96	0.266	− 1 (0.5)	0.46	− .69***
L. Verde	2792–5719	− 476	− 0.083	− 36.5 (0.0009)	0.18	− .42**
L. Blanca I	9–594	− 23.8	− 0.040	− 4.5 (0.02)	0.95	− .58***
C. del Inca	84–625	− 15.3	− 0.024	− 6.5 (0.01)	0.41	− .54***
L. Brava	499–2795	110	0.039	− 13.5 (0.06)	0.34	− .73***
Veladero	0.3–51	7.31	0.142	− 0.7 (0.01)	0.61	− .47**

Probability values: ***$p < 0.001$, **$p < 0.01$, *$p < 0.05$

used to estimate plant productivity. NDVI ranges from − 1 to 1 with extreme negative values representing water, average values (around zero) represent bare soil, and positive values representing vegetation. As in others regions of the Andean Puna, NDVI values in photosynthetically active vegetation of peatlands oscillate between 0.2 and 0.8, with average values of 0.66 (Aliaga and Callisaya 2012). We worked with the annual values of the large integrated value of NDVI: the area under the NDVI curve, estimated as the cumulative value of NDVI time series in vegetation growth during the growing season (Jonsson and Eklundh 2002; White et al. 2009) for the 2001–2012 period. NDVI annual integral is used as a descriptor of ecosystem functioning and a reliable indicator of the system productivity through the whole growing season (Tucker and Sellers 1986). To relate productivity with lake fluctuations, we chose the 50 nearest peatlands to each lake and within the same sub-watershed, based on distances computed between centroids of lakes and peatlands using Quantum GIS software. For each of these peatland groups, we calculated the annual average NDVI values and the NDVI data coefficient of variation (CV = standard deviation/mean) as a measure of the variation/stability of peatlands.

Precipitation

We used Tropical Rainfall Measuring Mission (TRMM) precipitation data 3B43 version 7 (3B43 v7), a multi-satellite precipitation monthly data with spatial resolution of 0.25° × 0.25°, available from 1998 onwards. TRMM data is freely provided by the NASA Goddard Earth Sciences Data and Information Services Center, and was obtained through the NASA Giovanni platform (https://giovanni.gsfc.nasa.gov/giovanni/). The data was created using TRMM-adjusted merged microwave-infrared precipitation rate (in mm/h.) and root-mean-square (RMS) precipitation-error estimates. For this study, we selected TRMM products that contain estimated precipitation data from 1998 to 2017. We worked with accumulated precipitation from November before each lake water body area measurement, until May of the next year. We chose to use data from November to ensure capturing the whole precipitation of the rainy season, technically starting in December. Winter precipitation was not included since it represents less than 20% of the annual precipitation and is likely subject to larger estimate errors. We extracted the accumulated precipitation value for each year of the time series using the centroid of each lake as a spatial reference.

Temperature

To obtain mean temperature values in each lake, we used the University of East Anglia CRU TS version 4.01 climate dataset (Harris et al. 2014), available for free through the CRU website (https://crudata.uea.ac.uk/cru/data/hrg/). The CRU TS 4.01 estimates are based on monthly observational data calculated from daily or sub-daily data by National Meteorological Services and other external agents; and contain data on many climatic variables covering Earth's land areas for the 1901–2016 period, in grids with 0.5° × 0.5° spatial resolution. We extracted the mean monthly temperature values at each lake location using the centroid of each lake as spatial reference, and then we calculated the mean annual temperature in each lake from 1986 to 2016.

Pacific climatic influences on lakes

We used the multivariate ENSO index (MEI) as the index of Pacific climate variability to analyze the climate influence of the Pacific Ocean on lake fluctuations. MEI is calculated on a bimonthly basis, and it is the first principal component of six main observed variables over the tropical Pacific (Wolter and Timlin 1993): sea level pressure, zonal and meridional components of the surface wind, sea surface temperature, surface air temperature, and sky cloudiness (Hanley et al. 2003). As computed by Wolter and Timlin (1993, 1998), MEI is available online from 1950 onwards (https://www.esrl.noaa.gov/psd/enso/mei/table.html). Higher values of the index indicate the presence of El Niño condition, while lower values indicate the presence of La Niña events. Among the various indices that describe ENSO phenomenon, MEI has proven to be the most useful index, mainly because it synthesizes six representative meteorological variables (Mazzarella et al. 2013). We used the index values from May–June bimester of the year before the lake measurement until the April–May bimester of the year in which the lakes were measured. We afterwards summed all the bimesters to use a single value, since this reflects the present conditions (El Niño or La Niña) throughout each analyzed year.

Statistical analysis

To describe relationships between fluctuations in lake water body area we used the interannual water body area fluctuation matrix to calculate correlations of the resulting time series. To explore relations between peatlands productivity and lakes, we correlated annual average NDVI values and NDVI CV values for each peatlands group against the corresponding lake water body area.

Correlations of climatic variables (precipitation, temperature and MEI index) with lake water body area and peatlands productivity were also evaluated. Additionally, we report correlations between annual precipitation and mean annual temperature.

For a better understanding of the time periods analyzed for each variable and the type of correlation used, see Fig. 2. All correlation analyses for all variables were performed in the statistical software R Version 1.1.453.

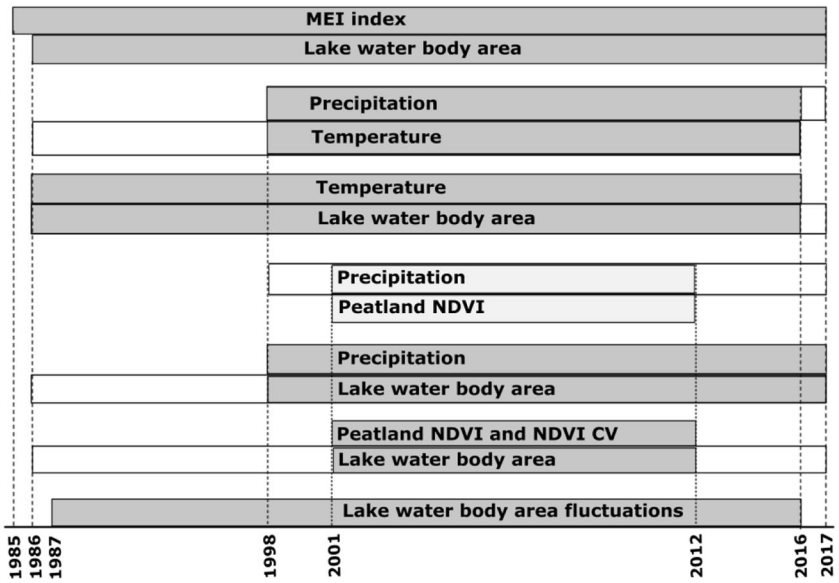

Fig. 2 Time framework of the different analyses. Shaded areas in each variable bar indicate the time period for which the correlation was analyzed. Dark gray indicates the Pearson correlation and light gray indicates the Spearman correlations between variables

Results

Clustering, lake trends and water body area fluctuations

The HC analysis performed resulted in two main clusters were lake fluctuations varied in a comparatively synchronous fashion (Fig. 3a). These clusters discriminated two major geographic zones along the northeast-southwest gradient of the study area (Fig. 3b). The northeast-center zone/cluster (NE Cluster) includes Pozuelos, Vilama, Salinas Grandes, Rio Grande, Hombre Muerto, Diamante, Carachipampa, Laguna Blanca, and Incahuasi lakes. The south-western zone/cluster (SW Cluster) includes Antofalla, Laguna Verde, Laguna Blanca I, Corona del Inca, Laguna Brava, and Veladero lakes. Additionally, we found that water body area fluctuations in Salinas Grandes and Rio Grande lakes (NE cluster) correlate negatively

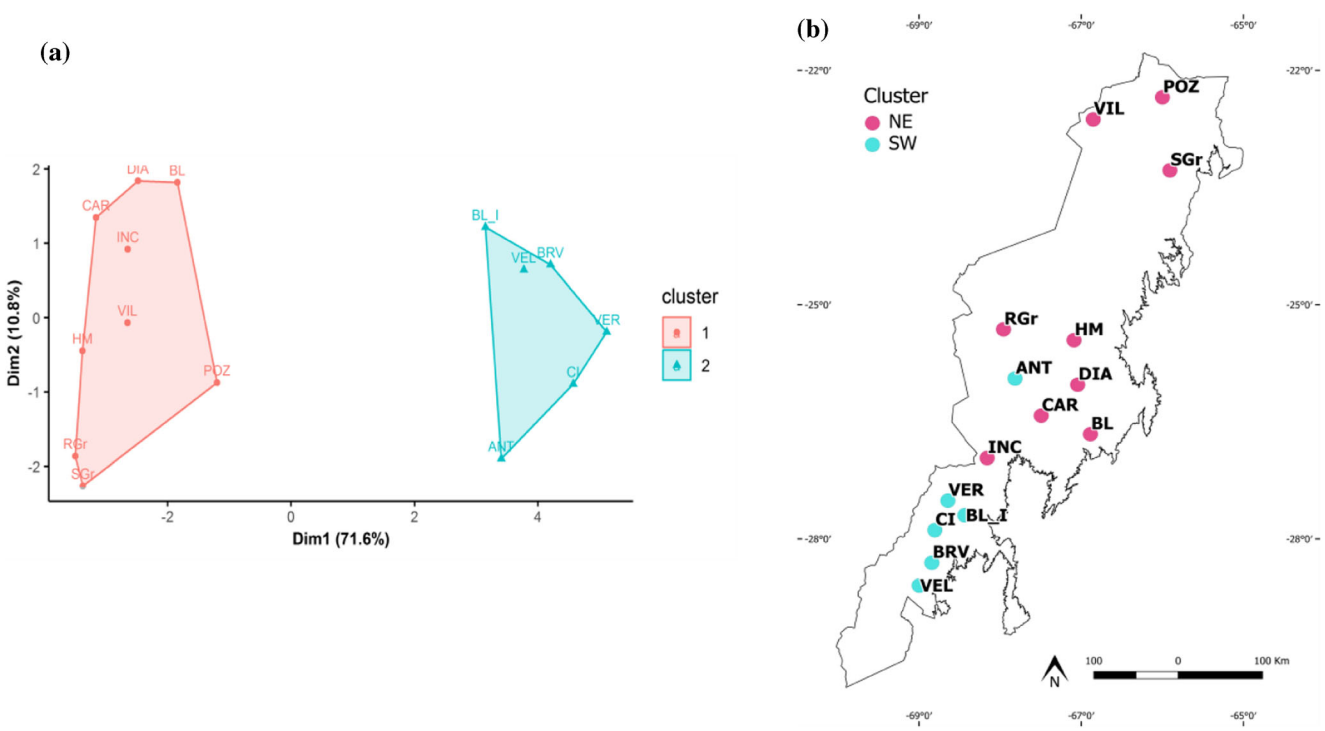

Fig. 3 **a** Plot of the two clusters of lakes identified according to their water body area fluctuations similarity. Axes show the two principal components that explain most of the data variation; **b** map of the spatial distribution of the lakes color-coded by cluster 1 (NE), and 2 (SW)

with most of the SW cluster lakes (Table 1 in online supplement).

Consistently with a regional pattern towards drier conditions, the general trend was a reduction in lake water body area (− 68.43 ha/year, $p = 0.67$ in NE cluster; and − 50.83 ha/year, $p = 0.01$ in SW cluster), but there was great interannual water body area variability. Four lakes actually showed a water body area increase: Salinas Grandes, Hombre Muerto, and Laguna Blanca in NE Cluster (11.4, 5.8 and 5.9 ha/year respectively); and Antofalla within SW Cluster (10.8 ha/year) which was the lake with the more pronounced water body area increase (Table 2, Fig. 4). The most common, negative trends, included Pozuelos, Vilama, Rio Grande, Diamante, Carachipampa, and Incahuasi lakes in NE Cluster; and Laguna Verde, Laguna Blanca I, Corona del Inca, Laguna Brava, and Veladero in SW Cluster. Among the group of lakes with water body area reduction trends, Diamante (NE Cluster), Laguna Brava, and Laguna Verde (SW Cluster) were the ones that experienced a stronger reduction (− 12.9, − 13.5, and − 36.5 ha/year, respectively). Lakes with larger water body area experienced higher negative fluctuations (i.e., area decrease). Many lakes had very small minimum area and were even completely dry in one or more years in the time series, such as Pozuelos (years 1994 and 1995), Salinas Grandes (years 1992, 1994, 1995, 1996, 1998, 2000, 2003, 2004, 2016 and 2017) and Laguna Blanca (years 1996, 2003, 2007, 2010, 2015 and 2016) of NE Cluster; and Antofalla (year 1987) of SW Cluster. These last three lakes also showed a trend to increase in water body area throughout the period studied.

Interannual fluctuations in water body area of all lakes studied were mostly positively and significantly correlated between different lakes (Table 1 in online supplement), suggesting that they overall respond to a common climate control. Almost 85% of the pairwise correlations were positive; 36% were higher than 0.4, of which in 54% the statistical significance was < 0.001 (Table 1 in online supplement).

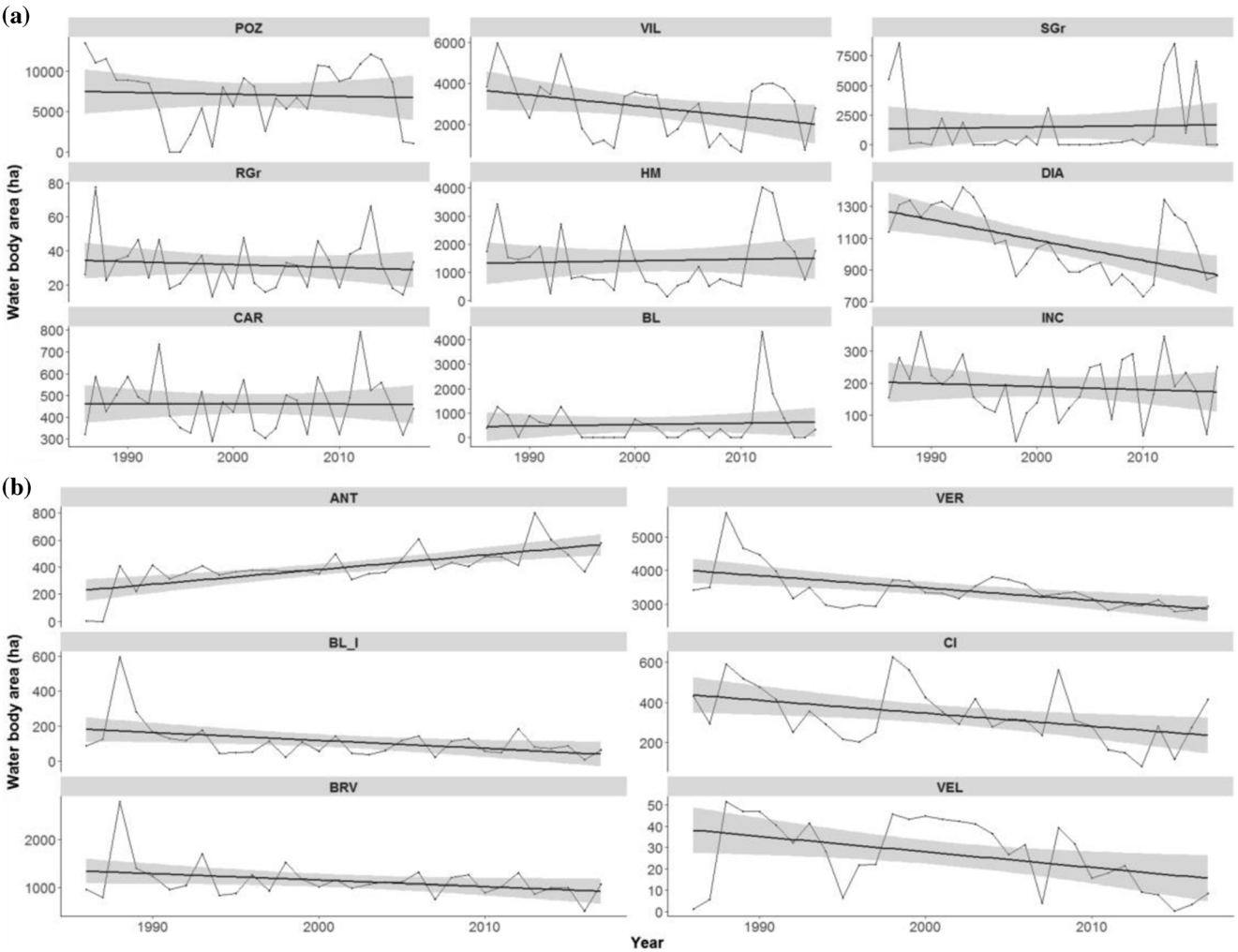

Fig. 4 Trends in lake water body area through the time series. **a** Trends in lakes grouped in NE Cluster; **b** trends in lakes grouped in SW cluster

Peatland productivity, lake water body area, and precipitation

Correlations between lake water body area and peatland phenological parameters over time were also variable (Table 3). In general, correlations were positive in both clusters. Pozuelos and Incahuasi (NE Cluster, $r = 0.80$, $p = 0.003$ and $r = 0.80$, $p = 0.003$, respectively); and Laguna Brava and Laguna Verde (SW Cluster, $r = 0.68$, $p = 0.018$, and $r = 0.55$, $p = 0.06$, respectively) showed strong and significant correlations. In Corona del Inca (Cluster SW), the correlation was negative, but weak and non-significant. A similar situation occurred regarding the NDVI CV values: overall, CV was negatively associated with lake area, but this relationship was significant only in Pozuelos (Cluster NE) (Table 3). Thus, in lakes with larger water body area, the NDVI values of peatlands remained more stable (had lower CV). Correlations between peatland NDVI and TRMM precipitation estimates was always non-significant, with both positive and negative values and weaker values than the correlations between lake water body area and peatland productivity (Table 3). Relationships between lake water body area and peatland NDVI were relatively consistent: 14 of the 15 lakes showed positive correlations with peatland NDVI being CI the unique lake with negative correlation. On average, the positive correlation values were > 0.3, and four of these were statistically significant.

TRMM precipitation and lake water body area

The relationship between TRMM accumulated precipitation and lake water body area showed a high variability between clusters. We found positive correlations in most of the lakes of NE cluster: Pozuelos, Vilama, Salinas Grandes, Hombre Muerto, Diamante, Carachipampa, Incahuasi, and Laguna Blanca I; and only in Corona del Inca in SW cluster (Table 3). However, correlation was strong and significant only in Pozuelos ($r = 0.72$, $p = 0.0005$) but weaker and generally non-significant in the others. We found negative correlations within NE cluster in Rio Grande, and Laguna Blanca; and Antofalla, Laguna Verde, Laguna Brava, and Veladero in SW Cluster (Table 3). These correlations were also weak; Laguna Verde was the only one showing a significant correlation ($r = -0.48$, $p = 0.038$).

CRU temperature data and lake water body area

Correlations between mean annual temperature and lake water body area did not show strong nor significant results (Table 2 in online supplement). However, two lakes located above 4000 m a.s.l. (Incahuasi 4002 m a.s.l, and Corona del Inca 5495 m a.s.l.), showed correlation values that approximate significance ($r = 0.32$, $p = 0.07$ and $r = -0.34$, $p = 0.06$, respectively). Correlations between precipitation

Table 3 Variables associations between lakes studied. From left to right: r and p values of the correlations between: NDVI and lake water body area; NDVI CV and lake water body area; NDVI and TRMM precipitation in peatlands; lake water body area and TRMM precipitation in each lake; NDVI average and NDVI CV values; and lake CV value. Significant correlations are indicated in italics

Lakes	NDVI–lake water body area		CV (NDVI)–lake water body area		NDVI–TRMM precipitation (peatland)		Lake water body area–TRMM precipitation (lake)		NDVI		Lake CV
	r	*p*	*r*	*p*	*r*	*p*	*r*	*p*	Mean	CV	
POZ	*.80*	*.003*	*−.60*	*.04*	.78	.92	*.72*	*.0005*	17616	0.40	0.54
VIL	.04	.89	.24	.44	−.28	.91	.11	.65	16684	0.53	0.50
SGr	.31	.32	.35	.26	.30	.80	.28	.25	15904	0.43	1.79
RGr	.15	.64	−.48	.11	.32	.88	−.12	.62	14126	0.49	0.47
HM	.23	.46	.36	.24	.27	.64	.16	.51	12210	0.57	0.74
ANT	.17	.60	−.17	.59	.43	.39	−.04	.86	10874	0.51	0.37
DIA	.39	.20	−.20	.53	−.02	.93	.11	.67	11044	0.88	0.19
CAR	.15	.64	−.17	.59	−.14	.23	.21	.38	18068	0.52	0.27
BL	.22	.49	.15	.62	−.24	.81	−.09	.72	17710	0.74	1.54
INC	*.80*	*.003*	−.38	.22	.02	.73	.18	.45	15282	0.48	0.46
VER	*.55*	*.06*	−.09	.76	−.25	.82	*−.48*	*.038*	15192	0.56	0.18
BL_I	.45	.14	−.50	.10	−.24	.95	.18	.45	15094	0.54	0.95
CI	−.22	.50	−.30	.33	−.10	.62	.13	.60	11654	0.56	0.41
BRV	*.68*	*.018*	.13	.67	.33	.86	−.07	.77	15346	0.45	0.34
VEL	.14	.66	−.20	.53	.15	.37	−.10	.68	16423	0.57	0.61

and temperatures were negative in 13 of the 15 lakes and significant in 5 of them (Table 2 in online supplement).

MEI index correlation with lake water body variability

There was a general negative relationship between lake water body area and the MEI index, and this was stronger in NE Cluster than in SW Cluster (Fig. 5). In the NE cluster, 5 of 9 lakes had correlation values lower than − 0.20 being the most negative − 0.40 (Pozuelos); while in the SW cluster only Veladero barely exceeded this value with − 0.21. Correlations between lake water body area and MEI index were mostly weak, negative and non-significant in almost all the NE cluster lakes, with the exception of Salinas Grandes and Diamante, which showed weak but positive and non-significant correlations with the index. The same trend was found within SW Cluster, where all lakes showed weak, negative and non-significant correlations (Fig. 5); with the exception of Laguna Verde, which has positive but still weak and non-significant correlation. The only lakes in which the correlations were stronger and approximated statistical significance are Pozuelos and Incahuasi (both in NE cluster).

Discussion

The general 1986–2017, but relatively weak, climatic trend towards aridization found in this study for the Puna ecoregion of Argentina is consistent with previous studies conducted in northern areas of the region (Carilla et al. 2013; Morales et al. 2015). In addition, aridity conditions have been identified in the Central Andes of South America (Boucher et al. 2011); as well as reductions of glaciers in the Tropical Andes (Francou et al. 2003; Vuille et al. 2008) in association with the regional increase in temperature (Vuille et al. 2000; Urrutia and Vuille 2009). The division of lakes into two major geographic zones (NE and SW clusters) shows that lakes fluctuate in response to local climate conditions that were not previously evident, and that emerge as a clear pattern in this study. Within NE cluster, 6 of 9 lakes showed a trend towards water body area reduction, while in SW Cluster, 5 of 6 lakes showed this trend. Certain lakes, such as Diamante and Laguna Verde (medium and large area lakes respectively) were more stable, with smaller CV and with water cover during all the years. These lakes appear have greater ecological stability and resilience to extreme climatic events; in opposition to other lakes that showed very pronounced area changes and became completely dry during one or more years; such as Salinas Grandes, Pozuelos and Laguna Blanca. However, Diamante and Laguna Verde experience a stronger water body area reduction according to their average water body area (Diamante − 12.9 ha/year and Laguna Verde − 36.5 ha/year). Then, possibly lake water body area changes reflect the complexity of the watershed behavior that may include both superficial and underground water sources that do not follow linearly the overall climatic pattern; for example, rivers coming from the Eastern side of the Puna, likely related to a different climatic system (Jobbágy et al. (2011)). Overall, largest lakes are in larger watersheds with more complex ecosystems and environments, which could result in higher stability and resilience to climate change (Dong et al. 2018); as it could be the case of Laguna Verde and Vilama here studied.

The relationship found between lake water body area and their fluctuations indicates that larger lakes lose more water, since the fluctuations are larger and negative. Given that evaporation is considered the main water output of lakes with no drainage (Brakenridge 1978; Currey and Sack 2009), larger lakes would have more water area available for evaporation (Grasso 1996). This is particularly reasonable for the lakes here studied, since they are shallow lakes with average depth 4.5 m; being only Corona del Inca the one that exceeds this value by almost 8 m (Messager et al. 2016).

Lake water body area was positively related to the productivity of the nearby peatlands, although this relationship was only significant in Pozuelos (Cluster NE) and Laguna Brava (Cluster SW). This statistical weakness may be due to the fact that, due to the soil-plant-water feedbacks in which they base their existence (Belyea and Clymo 2001), peatlands are much more stable systems than lakes, have water regulation capacity, and depend strongly on groundwater (Squeo et al. 2006); which derives in more stable availability of water. This is apparent when observing the CV values of peatland NDVI versus lake water body area CV values (Table 3), with Salinas Grandes and Laguna Blanca as the most remarkable examples. However, in extreme years, the effect of droughts on the productivity values of peatlands stands out. The inverse relationship between NDVI CV and lake area implies that NDVI values become more stable (lower CV) as lake area increases; which could be an indicator of greater water availability, and a certain degree of association between these wetlands.

The generally weak, positive relationship between precipitation and lake water body area may be indicating that, at least during the rainy season, lake water body area could be more related to climatic variables affecting water balance other than precipitation; as high solar radiation or wind; which lead to higher evaporation rates. Probably as important, precipitation and lake water body area relationship might be indicating that climate spatial modeling is poor, mainly due to the paucity of instrumental records; this idea is reinforced by the fact that the strongest correlation between lake water body area and precipitation occurred in Pozuelos, the closest lake to the meteorological station of La Quiaca, which has the best instrumental record in the region. It is worth mentioning that in a few cases (e.g., Laguna Verde), negative associations between precipitation and lake water body area were also found, and this

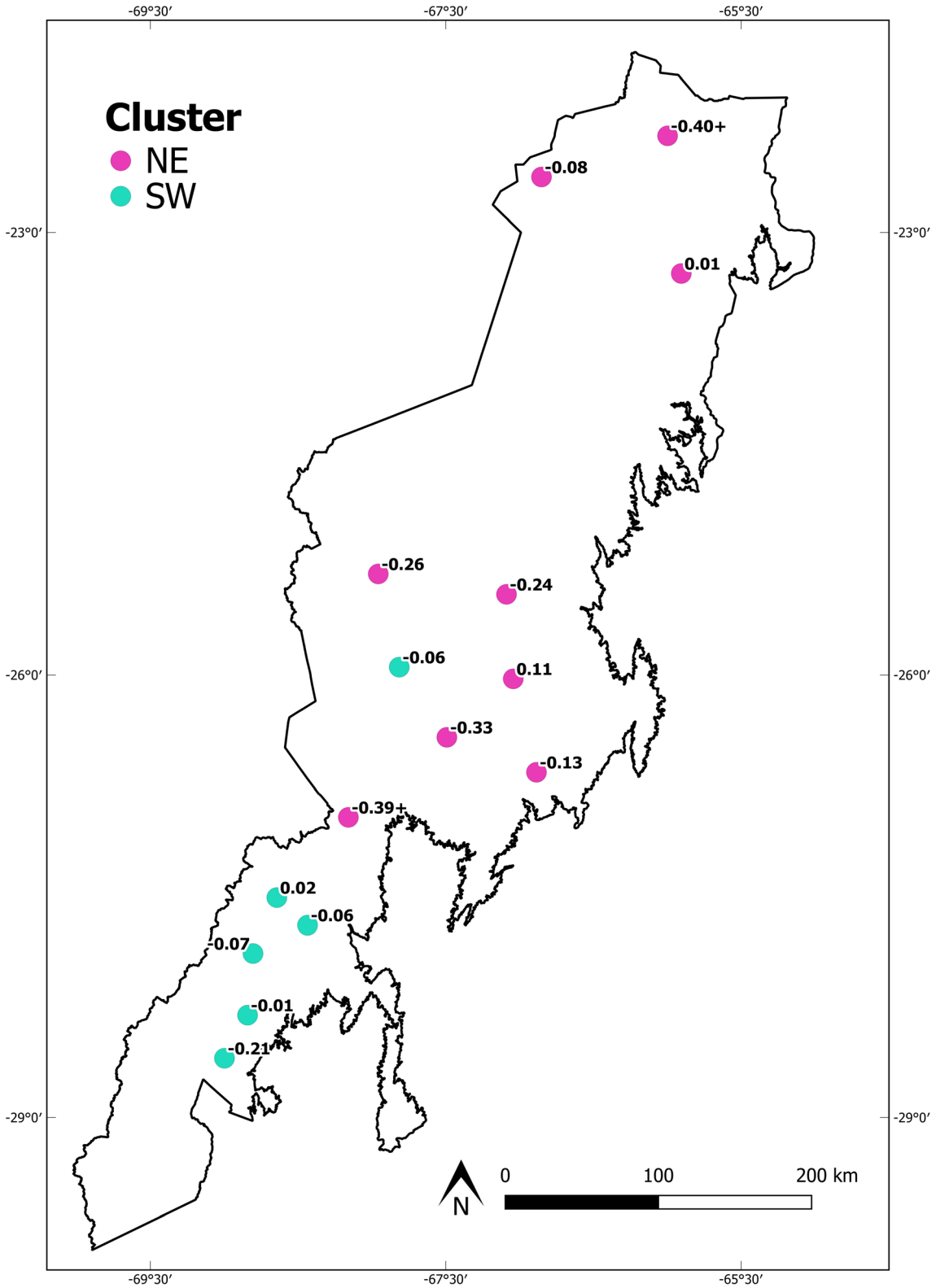

Fig. 5 Lakes map (color coded by clusters) indicating the correlation value between lake water body area and the MEI index. Symbol + indicates *p* values exceeding the 0.01 threshold

could be due to multiple causes, such as the climatic variables leading to higher evaporation rates, as mentioned above. Regarding the influence of temperature on lakes, the lack of correlation between mean annual temperature and lake water body area, but the negative relationship between temperature and precipitation, allows us to partially affirm that lake water

body area variations that could be explained by temperature are already explained by precipitation; as both variables are negatively correlated. Further, although there was no statistical significance, in general, the NE cluster lakes (except Pozuelos) were positively associated with temperatures; while the SW cluster lakes did it negatively (except Antofalla), again indicating the separation of the NE and SW geographic zones. As for precipitation, the meteorological stations used to interpolate temperature data are distant and located at a much lower altitude than the study region (except for La Quiaca); so these results may not correctly reflect the relationship between these variables. In addition, our findings suggest that other variables not studied here might be influencing lake water body area, since lakes are fed by other water sources, such as the melting of snow, which could have precipitated during the previous winter, and therefore it was not counted in the precipitation model used in this study. This issue should be further explored, considering that in the region snow usually does not accumulate in glaciers but in relatively ephemeral snowfields. Also, there might be confounding effects that we did not quantify, such as the influence of groundwater levels and land-uses over the catchment (Webster et al. 2000).

Relationships between lake water body area and the MEI index of ENSO were mostly weak. In both clusters, lake water body areas tended to decrease/increase their surface during El Niño/La Niña years, coinciding with that documented in previous studies for the High Andes (Garreaud and Aceituno 2001; Vuille and Keimig 2004). However, this situation was generally stronger in NE Cluster. Within SW Cluster, lake water body area dynamics seem to be even less influenced by the ENSO phenomenon. This lower influence of ENSO on the southwest lakes could be explained by the distance between the tropical Pacific and this part of the Puna, which might soften the effect of the phenomenon. Instead, this southern region could be more influenced by the Atlantic Anticyclone (Jobbágy et al. 2011). For a more complete and accurate interpretation of lake behavior in the region, it is necessary to separate the effects of non-climatic stressors from the effects caused by climatic oscillations, such as the ENSO phenomenon addressed in this study.

Conclusions

This study represents the first temporal analysis of the interannual area variability of the main lakes in the Puna region of Argentina, using Landsat images acquired for more than three decades. It contributes to a better understanding of ranges of variability of wetlands as key ecosystems in a high elevation desert region, and of the climatic forces that influence lake dynamics in a region characterized by a lack of climate data. We found that lakes are grouped in two clusters of relatively synchronic area variability and association with ENSO indices; and that these clusters define two main geographic zones: NE and SW. Consistently with previous observations of an overall aridization trend, both large spatial and interannual variability indicates that individual watersheds play a key role in defining wetland dynamics. Overall, however, lake fluctuations show high individual variability and much of it is unexplained by the climate models here used.

The study applies tools for assessing ecological stability and resilience of lakes (a key regional ecological feature) to climate variability, and for predicting peatland productivity (the key wetlands for the ecological functioning of arid highland environments), which is stronger than climate models. With these tools, we can reach a better understanding about the future of high mountain wetlands; and their vulnerability to climate change and human uses. This can serve specifically for decision-making aiming at the conservation (e.g., Argentine National Wetlands Law Bill) and management (e.g., management plans for anthropic activities) in these regions, where water is a limiting ecological factor. For a better understanding of climate-driven changes and their implications for ecosystems, it is necessary to further explore the integration of many aspects upon which these changes depend, such as land-use (including mining and urbanization) a historical and actual driver of ecological and social changes in the Puna region.

Acknowledgments We would like to thank USGS for providing access to the Landsat image archive, and Google for providing the space in the cloud that made it possible to analyze a large amount of data. Thanks to Sofía Nanni for her contribution in reviewing the English language of this work.

Funding information This work was funded by the CONICET, Grants from PICT2012-1565 FONCYT and PICT 2016-2173 FONCYT to RG, EC, CN and AI; and Rufford Small Grants 81430c-1 to EC.

References

Aliaga CB, Callisaya JF (2012) Estudio espacial multitemporal de variaciones en superficie observadas a través de imágenes satelitales Landsat en una región del Parque Nacional Sajama Bolivia. Report. Project: Adaptación al cambio climático en comunidades Andinas bolivianas que dependen de glaciales tropicales. La Paz, Bolivia: Agua Sustentable

Belyea LR, Clymo RS (2001) Feedback control of the rate of peat formation. Proc R Soc Lond B Biol Sci 268(1473):1315–1321. https://doi.org/10.1098/rspb.2001.1665

Beniston M (2003) Climatic change in mountain regions: a review of possible impacts. In: Diaz HF (eds.) Climate variability and change in high elevation regions: past, present & future. Advances in global change research, vol 15. Springer, Dordrecht. https://doi.org/10.1007/978-94-015-1252-7_2

Beniston M (2005) Mountain climates and climatic change: an overview of processes focusing on the European Alps. Pure Appl Geophys 162(8–9):1587–1606. https://doi.org/10.1007/s00024-005-2684-9

Beniston M, Diaz H, Bradley R (1997) Climatic change at high elevation sites. An overview. Clim Chang 36(3–4):233–251. https://doi.org/10.1023/A:1005380714349

Boucher E, Guiot J, Chapron EA (2011) Millennial multi-proxy reconstruction of summer PDSI for southern South America. Clim Past 7: 957–974. https://doi.org/10.5194/cp-7-957-2011

Brakenridge GR (1978) Evidence for a cold, dry full-glacial climate in the American Southwest. Quat Res 9(1):22–40. https://doi.org/10.1016/0033-5894(78)90080-7

Buytaert W, Vuille M, Dewulf A, Urrutia R, Karmalkar AV, Celleri R (2010) Uncertainties in climate change projections and regional downscaling in the tropical Andes: implications for water resources management. Hydrol Earth Syst Sci 14:1247–1258. https://doi.org/10.5194/hess-14-1247-2010

Cabrera AL (1976) Regiones fitogeográficas argentinas. Editorial ACME, Buenos Aires, Argentina

Carilla J, Grau HR, Paolini L, Morales M (2013) Lake fluctuations, plant productivity, and long-term variability in high-elevation tropical Andean ecosystems. Arct Antarct Alp Res 45(2):179–189. https://doi.org/10.1657/1938-4246-45.2.179

Caziani S, Derlindati E (1999) Humedales altoandinos del noroeste de Argentina. Su contribución a la biodiversidad regional. In: Malvárez I (ed) Tópicos Sobre Humedales Subtropicales y Templados de Sudamérica. Montevideo, Uruguay. ORCYT, pp 1–13

Chander G, Markham BL, Helder DL (2009) Summary of current radiometric Calibration coefficients for Landsat MSS, TM, ETM+, and EO-1 ALI. Remote Sens Environ 113(5):893–903. https://doi.org/10.1016/j.rse.2009.01.007

Currey DR, Sack D (2009) Hemiarid lake basins: hydrographic patterns. In Parsons AJ, Abrahams AD (eds.) Geomorphology of desert environments, Springer: Dordrecht, Netherlands, pp. 489–514. https://doi.org/10.1007/978-1-4020-5719-9_16

Dong S, Peng F, You Q, Guo J, Xue X (2018) Lake dynamics and its relationship to climate change on the Tibetan Plateau over the last four decades. Reg Environ Chang 18(2):477–487. https://doi.org/10.1007/s10113-017-1211-8

Farías ME, Rascovan N, Toneatti DM, Albarracín VH, Flores MR, Poiré DG, Collavino M, Aguilar OM, Vázquez MP, Polerecky L (2013) The discovery of stromatolites developing at 3570 m above sea level in a high-altitude volcanic lake Socompa, Argentinean Andes. PLoS One 8(1):e53497. https://doi.org/10.1371/journal.pone.0053497

Francou B, Vuille M, Wagnon P, Mendoza J, Sicart JM (2003) Tropical climate change recorded by a glacier in the Central Andes during the last decades of the twentieth century: Chacaltaya, Bolivia, 16°S. J Geophy Res 108(D5). https://doi.org/10.1029/2002JD002959

Garreaud R, Aceituno P (2001) Interannual rainfall variability over the South American Altiplano. J Clim 14(12):2779–2789. https://doi.org/10.1175/1520-0442(2001)014<2779:IRVOTS>2.0.CO;2

Glantz MH, Katz RW, Nicholls N (1991) Teleconnections linking worldwide climate anomalies: scientific basis and societal impact, vol 535. Cambridge University Press, Cambridge

Grasso DN (1996) Hydrology of modern and late Holocene lakes, Death Valley, California. Water-resources investigations report 95-4237, USGS Numbered Series. U.S. Dept. of the Interior, U.S. Geological Survey: Information Services, Denver, Colorado, United States https://doi.org/10.3133/wri954237

Hanley DE, Bourassa MA, O'Brien JJ, Smith SR, Spade ERA (2003) Quantitative evaluation of ENSO indices. J Clim 16(8):1249–1258. https://doi.org/10.1175/1520-0442(2003)16<1249:AQEOEI>2.0.CO;2

Harris I, Jones PD, Osborn TJ, Lister DH (2014) Updated high-resolution grids of monthly climatic observations—the CRU TS3.10 dataset. Int. J. Climatol. 34(3):623–642. https://doi.org/10.1002/joc.3711

Haylock MR, Peterson TC, Alves LM, Ambrizzi T, Anunciação YMT, Baez J, Vincent LA, Barros VR, Berlato MA, Bidegain M, Coronel G, Corradi V, Garcia VJ, Grimm AM, Karoly D, Marengo JA, Marino MB, Moncunill DF, Nechet D, Quintana J, Rebello E, Rusticucci M, Santos JL, Trebejo I, Vincent LA (2006) Trends in total and extreme South American rainfall in 1960-2000 and links with sea surface temperature. J Clim 19(8):1490–1512. https://doi.org/10.1175/JCLI3695.1

Hsu CW, Chang CC, Lin CJ (2007) A practical guide to support vector classification. National Taiwan University

Izquierdo AE, Aragón R, Navarro CJ, Casagranda E (2018) Humedales de la Puna: principales proveedores de servicios ecosistémicos de la región. In HR Grau, MJ Babot, A Izquierdo y A Grau (eds.) La Puna argentina: naturaleza y cultura. Serie de Conservación de la Naturaleza Vol. 24, pp 96–111

Izquierdo AE, Foguet J, Grau HR (2015) Mapping and spatial characterization of argentine high Andean peatbogs. Wetl Ecol and Manag 23(5):963–976. https://doi.org/10.1007/s11273-015-9433-3

Izquierdo AE, Foguet J, Grau HR (2016) Hidroecosistemas de la Puna y Altos Andes de Argentina. Acta Geológica Lilloana 28(2):390–402

Jobbágy EG, Nosetto MD, Villagra PE, Jackson RB (2011) Water subsidies from mountains to deserts: their role in sustaining groundwater-fed oases in a sandy landscape. Eco Appl 21(3):678–694. https://doi.org/10.1890/09-1427.1

Jonsson P, Eklundh L (2002) Seasonality extraction by function fitting to time-series of satellite sensor data. IEEE Trans Geosci Remote Sens 40(8):1824–1832. https://doi.org/10.1109/TGRS.2002.802519

Kayastha N, Thomas V, Galbraith J, Banskota A (2012) Monitoring wetland change using inter-annual Landsat time-series data. Wetlands. 32(6):1149–1162. https://doi.org/10.1007/s13157-012-0345-1

Kusler J, Mitsch W, Larson J (1994) Humedales. Investigación y Ciencia 210:6–13

Latif M, Keenlyside NS (2009) El Niño/southern oscillation response to global warming. PNAS. 106(49):20578–20583. https://doi.org/10.1073/pnas.0710860105

Lee KS, Kim TH, Yun YS, Shin SM (2001) Spectral characteristics of shallow turbid water near the shoreline on inter-tidal flat. Korean J Remote Sens 17(2):131–139

Liebmann B, Fu R, Camargo S, Seth A, Marengo J, Carvalho L, Allured D, Vera C (2007) Onset and end of the rainy season in South America in observations and the ECHAM 4.5 atmospheric general circulation model. J Climate 20(10):2037–2050. https://doi.org/10.1175/JCLI4122.1

Lupo L, Morales M, Yacobaccio HD, Maldonado A, Grossjean M (2007) Cambios ambientales en la Puna jujeña durante los últimos 1200 años: explorando su impacto en la economía pastoril. In UNJu (eds.) Actas XVI Congreso Nacional de Arqueología Argentina Tomo III, San Salvador de Jujuy, Argentina, pp. 151–156

Mantero P, Moser G, Serpico SB (2005) Partially supervised classification of remote sensing images through SVM-based probability density estimation. IEEE Trans Geosci Remote Sens 43(3):559–570. https://doi.org/10.1109/TGRS.2004.842022

Mazzarella A, Giuliacci A, Scafetta N (2013) Quantifying the multivariate ENSO index (MEI) coupling to CO2 concentration and to the length of day variations. Theor Appl Climatol 111(3–4):601–607. https://doi.org/10.1007/s00704-012-0696-9

Meneses R, Loza Herrera S, Domic A, Palabral-Aguilera A, Zeballos G, Ortuño T (2015) Bofedales altoandinos. In Moya M, I Meneses R, Sarmiento J (eds.) Historia Natural de un Valle en Los Andes: La Paz, Segunda edición en español. Museo Nacional de Historia Natural: La Paz, Bolivia, pp. 191-205

Messager ML, Lehner B, Grill G, Nedeva I, Schmitt O (2016) Estimating the volume and age of water stored in global lakes using a geostatistical approach. Nat Commun 7:13603. https://doi.org/10.1038/ncomms13603

Mittermeier RA, Myers N, Thomsen JB, Da Fonseca GA, Olivieri S (2008) Biodiversity hotspots and major tropical wilderness areas: approaches to setting conservation priorities. Conserv Biol 12(3): 516–520. https://doi.org/10.1046/j.1523-1739.1998.012003516.x

Morales M, Carilla J, Grau HR, Villalba R (2015) Multi-century lake area changes in the southern Altiplano: a tree-ring-based reconstruction.

Clim Past 11(9):1821–1855. https://doi.org/10.5194/cp-11-1139-2015

Morales MS, Christie DA, Neukom R, Rojas F, Villalba R (2018) Variabilidad hidroclimática en el sur del Altiplano: pasado, presente y futuro. In HR Grau, MJ Babot, AE Izquierdo y A Grau (eds.), La Puna argentina: naturaleza y cultura. Serie de Conservación de la Naturaleza Vol. 24, pp 95–91

Müller H, Rufin P, Griffiths P, Barros Siqueira AJ, Hostert P (2015) Mining dense Landsat time series for separating cropland and pasture in a heterogeneous Brazilian savanna landscape. Remote Sens Environ 156:490–499. https://doi.org/10.1016/j.rse.2014.10.014

Paoli H, Bianchi AR, Yañez CE, Volante J N, Fernández DR, Mattalía MC, Noé YE (2002) Recursos Hídricos de la Puna, valles y Bolsones áridos del Noroeste Argentino. Convenio INTA EEA Salta-CIED

Philander SG (1989) El Niño, La Niña, and the southern oscillation. In International geophysics series, vol. 46, Academic Press, San Diego, CA, 293 pp.

Power S, Delage F, Chung C, Kociuba G, Keay K (2013) Robust twenty-first-century projections of El Niño and related precipitation variability. Nature. 502(7472):541–545. https://doi.org/10.1038/nature12580

Reboratti C (2005) Situación ambiental en las ecorregiones Puna y Altos Andes. In Brown A, Martinez Ortiz U, Acerbi M, Corcuera JF (eds.) La situación ambiental argentina, Fundación Vida Silvestre Argentina: Buenos Aires, Argentina, pp 33-51

Rokni K, Ahmad A, Selamat A, Hazini S (2014) Water feature extraction and change detection using multitemporal Landsat imagery. Remote Sens 6(5):4173–4189. https://doi.org/10.3390/rs6054173

Squeo FA, Veit H, Arancio G, Gutierrez JR, Arroyo MT, Olivares N (1993) Spatial heterogeneity of high mountain vegetation in the Andean desert zone of Chile. Mt Res Dev 13(2):203–209 https://www.jstor.org/stable/3673638

Squeo FA, Warner BG, Aravena R, Espinoza D (2006) Bofedales: high altitude peatlands of the central Andes. Rev Chil Hist Nat 79(2): 245–255 http://repositorio.uchile.cl/handle/2250/119990

Tucker CJ, Sellers PJ (1986) Satellite remote sensing of primary production. Int J Remote Sens 7(11):1395–1416. https://doi.org/10.1080/01431168608948944

Urrutia R, Vuille M (2009) Climate change projections for the tropical Andes using a regional climate model: temperature and precipitation simulations for the end of the 21st century. J Geophys Res 114: D02108. https://doi.org/10.1029/2008JD011021

Villagrán MC, Castro RV (1997) Etnobotánica y manejo ganadero de las vegas, bofedales y quebradas en el loa superior, Andes de Antofagasta, Segunda Región, Chile. Chungara Rev Antrop Chil 29(2):275–304

Vuille M, Bradley RS, Keimig F (2000) Interannual climate variability in the Central Andes and its relation to tropical Pacific and Atlantic forcing. J Geophys Res Atmos 105(D10):12447–12460. https://doi.org/10.1029/2000JD900134

Vuille M, Francou B, Wagnon P, Juen I, Kaser G, Mark B, Bradley R (2008) Climate change and tropical Andean glaciers: past, present and future. Earth-Science Review 89(3–4):79–96. https://doi.org/10.1016/j.earscirev.2008.04.002

Vuille M, Keimig F (2004) Interannual variability of summertime convective cloudiness and precipitation in the central Andes derived from ISCCP-B3 data. J Clim 17(17):3334–3348. https://doi.org/10.1175/1520-0442(2004)017%3C3334:IVOSCC%3E2.0.CO;2

Ward JH (1963) Hierarchical grouping to optimize an objective function. J Am Stat Assoc 58(301):236–244

Webster KE, Soranno PA, Baines SB, Kratz TK, Bowser CJ, Dillon PJ, Everett J, Hecky RE (2000) Structuring features of lake districts: landscape controls on lake chemical responses to drought. Freshw Biol 43(3):499–515. https://doi.org/10.1046/j.1365-2427.2000.00571.x

White MA, de Beurs KM, Didan K, Inouye DW, Richardson AD, Jensen OP, O'Keefe J, Zhang G, Nemani RR, van Leeuwen WJD, Brown JF, De Witt A, Schaepman M, Lin X, Dettinger M, Bailey AS, Kimball J, Schwartz MD, Baldocchi DD, Lee JT, Lauenroth WK (2009) Intercomparison, interpretation, and assessment of spring phenology in North America estimated from remote sensing for 1982–2006. Glob Chang Biol 15(10):2335–2359. https://doi.org/10.1111/j.1365-2486.2009.01910.x

Wolter K, Timlin MS (1993) Monitoring ENSO in COADS with a seasonally adjusted principal component index. In: Proceedings of the 17th climate diagnostics workshop, Norman, OK, NOAA/N MC/CAC, NSSL, Oklahoma Climate Survey. CIMMS and the School of Meteorology, University of Oklahoma, pp 52–57

Wolter K, Timlin MS (1998) Measuring the strength of ENSO events - how does 1997/98 rank? Weather. 53(9):315–324. https://doi.org/10.1002/j.1477-8696.1998.tb06408.x

Yeh SW, Kirtman BP (2007) ENSO amplitude changes due to climate change projections in different coupled models. J Clim 20(2):203–217. https://doi.org/10.1175/JCLI4001.1